Optical Response of Gas-Phase Atoms at Less than $\lambda/80$ from a Dielectric Surface

K. A. Whittaker,[1] J. Keaveney,[1,*] I. G. Hughes,[1] A. Sargsyan,[2] D. Sarkisyan,[2] and C. S. Adams[1,†]
[1]*Joint Quantum Centre (JQC) Durham-Newcastle, Department of Physics, Durham University, South Road, Durham DH1 3LE, United Kingdom*
[2]*Institute for Physical Research, National Academy of Sciences, Ashtarak 2, 0203, Armenia*
(Received 12 March 2014; revised manuscript received 6 May 2014; published 26 June 2014)

We present experimental observations of atom-light interactions within tens of nanometers (down to 11 nm) of a sapphire surface. Using photon counting we detect the fluorescence from of order one thousand Rb or Cs atoms, confined in a vapor with thickness much less than the optical excitation wavelength. The asymmetry in the spectral line shape provides a direct readout of the atom-surface potential. A numerical fit indicates a power law $-C_\alpha/r^\alpha$ with $\alpha = 3.02 \pm 0.06$ confirming that the van der Waals interaction dominates over other effects. The extreme sensitivity of our photon-counting technique may allow the search for atom-surface bound states.

DOI: 10.1103/PhysRevLett.112.253201 PACS numbers: 34.35.+a, 32.30.-r, 32.70.Jz

Atomic vapors are continuing to find new applications in quantum technologies such as chip-scale atomic clocks [1], magnetometry [2,3], magnetoencephalography [4], magnetocardiography [5], an atom-based optical isolator [6], quantum memories [7], frequency filtering [8,9], and in the field of nanoplasmonics (see Refs. [10,11] for reviews). As the miniaturization of these technologies progresses, many of these systems eventually reach the scale where the proximity of the atoms to a surface becomes significant. In this case a thorough understanding of the atom-surface interactions is essential. Many of the above applications use atoms in ground states or low-lying excited states, where the atom-surface (AS) interaction is relatively small as the induced dipole is only a few Debye. Even so, the AS interaction can still have a significant effect if the surface is in the near field of the atom, that is, within a fraction of the transition wavelength, λ, of the induced dipole. In this regime, the atom-surface potential is governed by an inverse power law $U_{\mathrm{vdW}} = -C_\alpha/r^\alpha$ where C_α is the coupling coefficient and r is the atom-surface distance. For an uncharged surface with $r < \lambda$ one expects a van der Waals interaction with $\alpha = 3$ [12]. However, if charges are present on the surface the Coulomb interaction may be larger than the van der Waals interaction, leading to a modification of α. The atom-surface potential is also strongly influenced by the presence of surface modes such as surface polaritons. However, for alkali atoms these couple more strongly to intermediate excited states where the energy level spacing is in the terahertz region [13–17]. Very close to the surface, bound states of the AS potential can be exploited, as recently demonstrated using He scattering from LiF surfaces [18]. The combination of bound states and surface resonances potentially allows guiding or trapping of atoms in close proximity to the surface [19]. This could lead to a new type of hybrid nanoscale atom-surface metamaterials, with atoms trapped in small channels that can be etched into any conceivable geometry, using focussed ion beam milling, for example [20].

The atom-surface interaction may be studied using a variety of methods. Scattering or deflection of an atom beam from a metallic surface [21–26], deflection of an ultracold atomic cloud from an atomic mirror [27,28] or diffraction of an atomic beam [29,30] have all been demonstrated. In these examples detection occurs after the interaction has taken place. For measurements of near-field effects at specific length scales such as atomic guiding, real-time *in situ* detection is preferable. Spectroscopic studies can be used, but come at the cost of probing a differential shift between two atomic states which both interact with the surface. The contribution from individual levels could be resolved using a multilevel excitation scheme, but that is not the focus of the present work. Considerable insight has been gained using frequency-modulated selective reflection spectroscopy in atomic vapors [31–34], which probes the vapor with a distance of order λ from the surface. Alternately, it is possible to investigate the AS interaction via atoms which are adsorbed on to a surface [35].

Although selective reflection spectroscopy is useful in determining the average shift from zero crossings, extracting detailed information from the line shape is complicated by the effects of dipole-dipole interactions between atoms, leading to self-broadening [36] and shifts [37], and for parallel surfaces the windows act as a low-finesse etalon which adds further complication to transmission and selective reflection signals [38,39].

In this work we detect fluorescence from an atomic vapor with nanoscale thickness, and use photon counting to probe

the atom-surface interaction at low atomic density where other interactions are negligible. This yields optimum resolution of the spectral line shape, which is a direct probe of the AS potential.

By fitting this high-resolution data to a comprehensive model of the atomic susceptibility, which has previously been used to model transmission and refraction in thermal temperature vapor cells in a range of experimental regimes [6,36,37,40–44], we extract the atom-surface interaction and thereby calibrate the position of an atom emitting at a particular frequency. Using this method, we are able to detect atoms within 10–15 nm of the dielectric surface. The possibility to exploit this length scale opens interesting prospects for strong coupling between atoms and nanoscale plasmonic structures or localized polaritons [19].

Figure 1 illustrates the general principle of our experiment, and the expected fluorescence line shapes. By confining the vapor between two surfaces, the interaction volume and hence the distribution of van der Waals shifts, as shown in Fig. 1(a), is independent of other variables such as the atomic density. The overall potential U_{vdW} (blue solid line) is the sum of both surfaces (dashed lines), and so has a minimum at the center of the cell, which quickly diverges at either surface. In the absence of the AS interaction, the fluorescence line shape is best approximated as a symmetric Lorentzian function (owing to Dicke narrowing, the

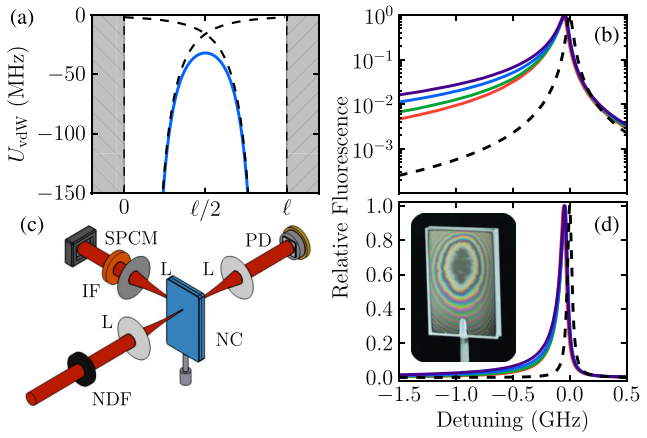

FIG. 1 (color online). (a) Atom-surface potential in the nanocell (NC) due to both walls (dashed lines) and combined (blue line). (b),(d) The effect of the atom-surface interaction on an initially Lorentzian spectral line (black dashed curves) is to shift the peak position, and create a pronounced asymmetry between the red and blue wings (red curves). The amount of asymmetry is a direct readout of the exponent α, as demonstrated by the four solid lines which are calculated with $\alpha = 4, 3, 2, 1.5$ (top to bottom). Panel (c) shows a schematic of the experimental setup used to detect off-axis fluorescence. NDF—neutral density filter; L—lens; NC—nanocell; IF—interference (bandpass) filter; PD—photodiode; SPCM—single photon counting module. Finally, a photo of the Cs nanocell used in the experiment is shown in the inset to panel (d). At the center of the Newton's rings interference pattern the thickness of the vapor column is 50 nm.

fluorescence line shape is not the usual Gaussian seen in conventional thermal vapor cells). The AS interaction causes an asymmetry in the fluorescence line shape, as shown in Figs. 1(b) and 1(d), and therefore gives a direct readout of the AS potential. This is most striking when shown on a log scale [panel (b)], though is also evident on a linear scale, where the shift of the peak is more obvious.

The experimental setup and the cell are illustrated in the Figs. 1(c) and 1(d) inset, respectively. The laser is scanned across resonance and fluorescence photons are counted on a single photon counting module to acquire a spectrum. In addition to the off-axis fluorescence, we also detect transmitted light; however, the amount of absorption at the densities considered in this work is small, typically $< 0.1\%$, so no useful signal is obtained. The cell photo, Fig. 1(d) inset, shows the characteristic Newton's rings interference pattern, and is indicative of varying vapor thickness. In the center of the rings we reach the minimum thickness of 50 nm, while at the edges of the cell the vapor thickness is maximum, around 2 μm. We can therefore tune the thickness by translating the cell with respect to the probe beam. The probe laser power is around 1 μW and the beam is focussed to a waist ($1/e^2$ radius) of 30 μm inside the cell. Both the dark count of the photon counting modules and the background count rate due to thermal photons from the heater accumulate at a constant rate and are uniformly distributed in time, and are therefore simply subtracted from the data during post-processing.

For spectroscopic reference and calibration, we also monitor the transmission of the laser light through a 7.5 cm vapor cell, and linearize the laser scan using a Fabry-Perot etalon, in the same way as our previous work [36,37,40]. More details on the photon counting technique can be found in Ref. [39].

Figure 2 shows fluorescence spectra in Rb vapor at various cell thicknesses. In panel (a) we show fluorescence from a vapor with thickness $\ell = 350$ nm, at a temperature $T = 85\,^{\circ}\mathrm{C}$ which corresponds to an atomic number density $N = 2 \times 10^{12}$ cm^{-3}. With this density and our beam geometry the laser interacts with on average around $\mathcal{N} = 900$ atoms at any one time; the vapor has a peak optical density $\sim 5 \times 10^{-3}$. Compared with the normal Doppler profile (grey area), the spectra are considerably narrower. After fitting to our model we extract a Lorentzian linewidth of 59 ± 1 MHz. At $\ell = 350$ nm (b) the AS interaction is negligibly small. In panels (b) and (c) we present data where the AS interaction is significant. At $\ell = 60$ nm spectral broadening due to reduced time-of-flight and dipole-dipole interactions (self-broadening) impairs resolution of individual hyperfine resonances, but a shift of the spectral features is noticeable, and is most pronounced on the two strongest (^{85}Rb) spectral features. At $\ell = 50$ nm (c), we reach the minimum width at which it is still possible to obtain a reasonable fit to the model. Here we use a lower temperature to reduce dipole-dipole interactions, but this

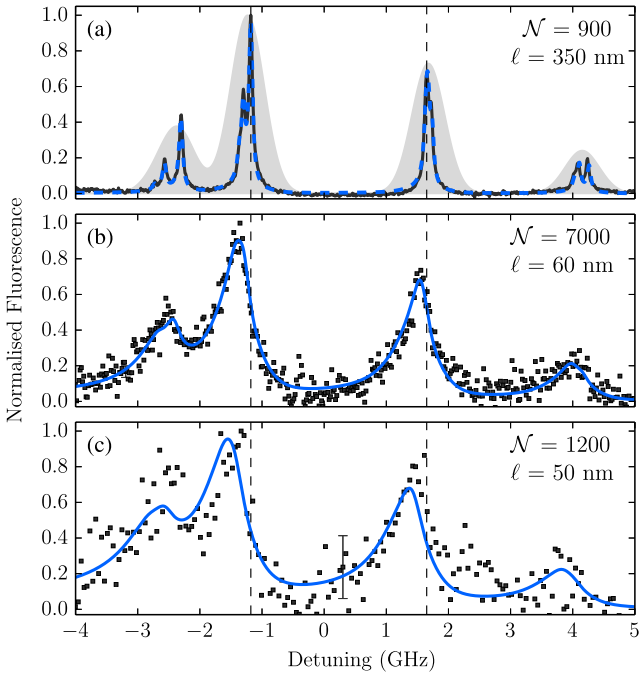

FIG. 2 (color online). (a) Fluorescence from a Rb vapor with thickness $\ell = 350$ nm at a temperature $T = 85\,^{\circ}\mathrm{C}$, integration time approximately 15 minutes. At this thickness the atom-surface interaction is negligible and owing to strong Dicke narrowing, the line shape of each hyperfine transition is well approximated by a Lorentzian with a (fitted) FWHM of 59 ± 1 MHz, and it is therefore possible to resolve each hyperfine transition. For comparison, the grey outline shows the fluorescence signal expected from a conventional Doppler-broadened vapor. (b) Fluorescence from a vapor with thickness $\ell = 60$ nm at a temperature $T = 150\,^{\circ}\mathrm{C}$, integration time approximately 1 hour. The atom-surface interaction significantly shifts the center of the fluorescence peaks, and because of the decreased time of flight of the atoms the lines are broadened. However, the linewidth is still narrower than the Doppler width. (c) Fluorescence from a vapor with thickness $\ell = 50$ nm at a temperature $T = 130\,^{\circ}\mathrm{C}$, integration time approximately 8 hours. Because of the thickness of the vapor and the reduced number density, the signal-to-noise ratio (SNR) is much weaker than in panel (b), even though the data have been binned more coarsely. However, a good fit to our theoretical model is still achieved. In this panel the asymmetry between red- and blue-detuned wings is most pronounced. In all panels, $\mathcal{N}$ is the mean number of atoms probed at any one time by the laser. Zero detuning represents the weighted center of the Rb $D2$ absorption line. The error bars shown [too small to be seen in panels (a) and (b)] are representative of the whole data array.

comes at the cost of a reduced signal-to-noise ratio (SNR). However, we still achieve a good fit. As the atoms are never more than 25 nm from a surface, both the shift and asymmetry of the spectral lines due to the AS interaction are significant.

While in principle one could extract a C_3 coefficient from the shift of the peak position relative to the unshifted position (black dashed line) this is difficult due to the many overlapping lines. A better approach is to fit the full spectral profile, which we do by fitting to our model with a floating C_3 parameter. The line shape is a convolution of the atomic response in free space with the surface potential, assuming a uniform distribution of atoms over the cell.

We vary the cell thickness from 50 nm to 390 nm ($\lambda/2$) to obtain many data sets like the ones in Fig. 2. By fitting all of the data with shared parameters, we extract an AS interaction strength $C_3 = 1.2 \pm 0.3\ \mathrm{kHz}\,\mu\mathrm{m}^3$ for the Rb $5S_{1/2} \rightarrow 5P_{3/2}$ transition. This is in reasonable agreement with a theoretical value of $1.8\ \mathrm{kHz}\,\mu\mathrm{m}^3$ (taken from Refs. [45,46] correcting for the surface reflectivity), and the relatively large error bar is probably due to the fact that each hyperfine transition has a slightly different dipole moment and thus a slightly different C_3 coefficient. However, fitting the data with 12 free interaction parameters instead of just one is computationally infeasible. Fitting these data with a surface potential of the form $-C_\alpha/r^\alpha$, where α is a floating parameter, allows the verification of the expected van der Waals r^{-3} power law. Fitting all our data we extract a weighted average $\alpha = 3.02 \pm 0.06$, confirming that there are no surface charges or other contaminants, and that the AS interaction follows the expected van der Waals form.

In contrast to the complexity of the Rb $D2$ line, the Cs $D1$ line is much simpler. In this system, the increased hyperfine splitting and the presence of only one isotope makes possible the investigation of individual hyperfine transitions. The ground state hyperfine splitting is over 9 GHz and the excited state hyperfine splitting is 1.17 GHz, still more than the Doppler width. Example data are shown in Fig. 3, for a cell thickness $\ell = 150$ nm at a temperature $T = 140\,^{\circ}\mathrm{C}$, corresponding to a Cs atomic density $N = 1.4 \times 10^{14}\ \mathrm{cm}^{-3}$. At this density, we expect the dipole-dipole interactions between atoms to contribute 11 MHz to the total linewidth. We extract from the fit a total Lorentzian linewidth of just (86 ± 1) MHz, and attribute the additional width to a time-of-flight broadening due to the cell geometry.

The relative narrowness of the peaks and good SNR means that we can detect shifts on the order of a few MHz with high precision, as shown in the inset of Fig. 3. In this case the shift of the peak is (20 ± 1) MHz. As we scan over only two transitions, the full spectral analysis including the AS interaction is much simpler, and for the data shown in Fig. 3 we achieve a reduced χ^2 parameter of 1.75, indicating an excellent fit [47].

Though the shift is clear from Fig. 3, the asymmetry in the line shape is not particularly apparent. In Fig. 4 we plot the same data on a logarithmic scale. The deviation in the red wing from the symmetric Lorentzian (black dashed line) is immediately apparent. In contrast, the theoretical model including AS interactions (red solid line) still matches the data well. For comparison, and in order to

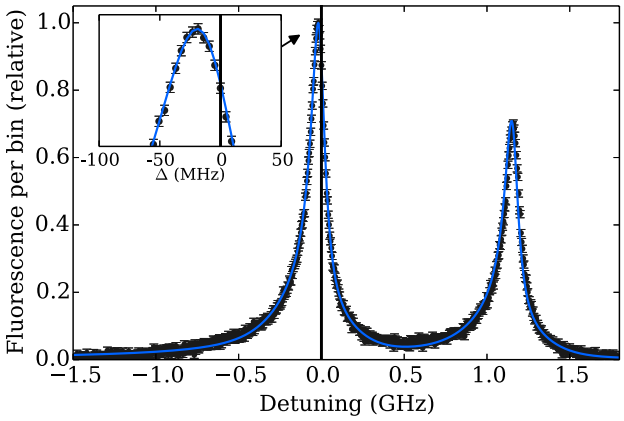

FIG. 3 (color online). Fluorescence from a Cs vapor with thickness $\ell = 150$ nm at a temperature $T = 140\,^{\circ}\mathrm{C}$, integration time approximately 8 hours. At this thickness the atom-surface interaction is small (20 ± 1 MHz peak shift), but measurable with this detection technique. Fitting these data to our model yields an excellent fit and from this we are able to extract a C_3 coefficient for the AS interaction (see main text). The Dicke narrowing is still particularly striking at this thickness—even though the atoms are at most 75 nm from the surface, the fitted linewidth is only 86 ± 1 MHz. Zero detuning is the resonance frequency of the Cs $6S_{1/2}\ F_g = 4 \rightarrow 6P_{1/2}\ F_e = 3$ transition.

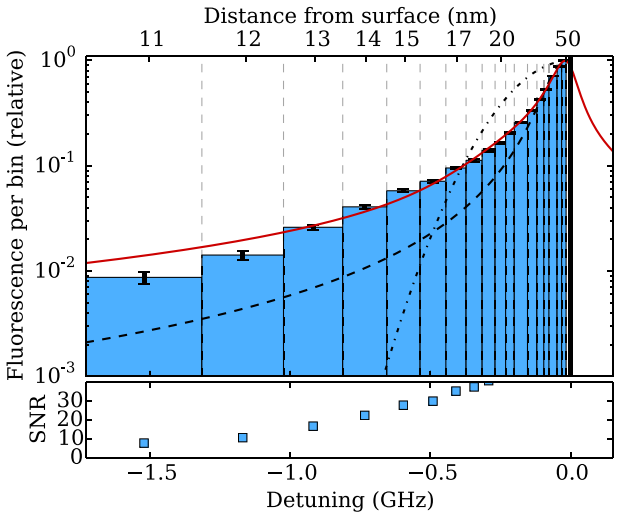

FIG. 4 (color online). Fluorescence data binned into nanometer steps. The raw data is the same as in Fig. 3. Whereas the asymmetry in the line shape may not be apparent from Fig. 3, when plotted on a log scale the difference from the symmetric Lorentzian (dashed black curve) is striking. The fluorescence at any given laser frequency detuning maps directly onto the distance of an atom from (either) one of the surfaces of the cell. By processing the photon arrival data into (uneven) frequency bins (blue bars, normalized by population density) whose width represents a distance ± 0.5 nm from the surface, we increase the effective signal-to-noise ratio (SNR). These data are clearly above that which would be expected from a standard Lorentzian resonance line (dashed black line), and confirms the detection of atoms within 11 nm of a sapphire surface. For these data we are limited by the scan range of the laser, not SNR. To rule out any effect of residual Doppler broadening in the wings, we also show a Gaussian response (dot-dashed line), which clearly does not fit the data. Near resonance Dicke narrowing means we do not observe the expected Doppler broadening, and far from resonance the Gaussian contribution is extremely small.

rule out any possible influence, we also plot the Gaussian contribution from Doppler broadening (dot-dashed line). At a detuning -1.5 GHz, the relative contribution of the Gaussian is expected to be of the order of 10^{-12} and is therefore completely negligible. Near resonance the normal Doppler profile is not observed due to Dicke narrowing.

Since the AS interaction maps atomic position to a frequency shift, we can interpret the fluorescence data as a direct readout of the atomic position in the cell. On the alternate axis in Fig. 4 we bin the data into nonuniform frequency steps such that the width of one bin corresponds to an atomic position change of 1 nm. Because the bins are so large in the wing of the resonance, this dramatically increases the SNR over the uniformly binned data in Fig. 3. From this, we can conclusively detect atoms (11.0 ± 0.5) nm away from a surface, since the signal level is many standard errors above that expected from the normal Lorentzian wing. Using the same procedure employed for Rb, we take a range of data where we vary the cell thickness between 80 nm and 200 nm and fit all the data with a combined C_3 parameter. From this, we extract a spectroscopic C_3 of (1.9 ± 0.1) kHz μm^3 between sapphire and the Cs $5S_{1/2} \rightarrow 6P_{1/2}$ transition, in agreement with previous work [31].

The reduced detection efficiency owing to the wavelength-dependent quantum efficiency of the single photon counting modules (SPCMs) and quality of bandpass filters available means that detecting Cs fluorescence is technically more difficult. The increased sensitivity to thermal photons produced in the cell heater also limits the maximum atomic density that is feasible to investigate using the current equipment. However, the main limit in the current experiment is how far we can scan the laser, not SNR. In future work we will investigate the region farther out in the red-detuned wing and look for a signature of atom-surface bound states, which have been predicted to occur at a detuning of around -20 GHz [48].

In conclusion, we have demonstrated a simple method for *in situ* detection of atoms a small fraction of a wavelength away from a dielectric surface, and used this method to investigate the AS interaction between sapphire and both Rb and Cs vapors in their first excited states. The spectral line shape is directly connected with the surface potential, and by analyzing the spectroscopic data we have both confirmed the expected $1/r^3$ power law and from this calculated the C_3 interaction strength coefficients for Rb and Cs. This technique could be used to probe long-range atom-surface bound states [48], or for the detection of atoms confined in nanocavities which could find

application as part of a micromechanical resonator system, similar to those in Ref. [49]. These topics will form the basis of future research.

The authors would like to thank K. N. Jarvis for experimental assistance, and acknowledge financial support from Durham University and EPSRC, grant reference EP/H002839/1.

*To whom all correspondence should be addressed.
james.keaveney@durham.ac.uk
†To whom all correspondence should be addressed.
c.s.adams@durham.ac.uk

[1] S. Knappe, V. Shah, P. D. D. Schwindt, L. Hollberg, J. Kitching, L.-A. Liew, and J. Moreland, Appl. Phys. Lett. **85**, 1460 (2004).
[2] W. C. Griffith, R. Jimenez-Martinez, V. Shah, S. Knappe, and J. Kitching, Appl. Phys. Lett. **94**, 023502 (2009).
[3] R. Mhaskar, S. Knappe, and J. Kitching, Appl. Phys. Lett. **101**, 241105 (2012).
[4] T. H. Sander, J. Preusser, R. Mhaskar, J. Kitching, L. Trahms, and S. Knappe, Biomed. Opt. Express **3**, 981 (2012).
[5] R. Wyllie, M. Kauer, G. Smetana, R. Wakai, and T. Walker, Phys. Med. Biol. **57**, 2619 (2012).
[6] L. Weller, K. S. Kleinbach, M. A. Zentile, S. Knappe, I. G. Hughes, and C. S. Adams, Opt. Lett. **37**, 3405 (2012).
[7] B. Julsgaard, J. Sherson, J. I. Cirac, J. Fiurášek, and E. S. Polzik, Nature (London) **432**, 482 (2004).
[8] R. P. Abel, A. K. Mohapatra, M. G. Bason, J. D. Pritchard, K. J. Weatherill, U. Raitzsch, and C. S. Adams, Appl. Phys. Lett. **94**, 071107 (2009).
[9] J. A. Zieliska, F. A. Beduini, N. Godbout, and M. W. Mitchell, Opt. Lett. **37**, 524 (2012).
[10] D. K. Gramotnev and S. I. Bozhevolnyi, Nat. Photonics **4**, 83 (2010).
[11] M. I. Stockman, Opt. Express **19**, 22029 (2011).
[12] H. B. G. Casimir and D. Polder, Phys. Rev. **73**, 360 (1948).
[13] H. Failache, S. Saltiel, M. Fichet, D. Bloch, and M. Ducloy, Phys. Rev. Lett. **83**, 5467 (1999).
[14] H. Failache, S. Saltiel, A. Fischer, D. Bloch, and M. Ducloy, Phys. Rev. Lett. **88**, 243603 (2002).
[15] H. Failache, S. Saltiel, M. Fichet, D. Bloch, and M. Ducloy, Eur. Phys. J. D **23**, 237 (2003).
[16] H. Kübler, J. P. Shaffer, T. Baluktsian, R. Löw, and T. Pfau, Nat. Photonics **4**, 112 (2010).
[17] A. González-Tudela, P. A. Huidobro, L. Martín-Moreno, C. Tejedor, and F. J. García-Vidal, Phys. Rev. Lett. **110**, 126801 (2013).
[18] M. Debiossac, A. Zugarramurdi, P. Lunca-Popa, A. Momeni, H. Khemliche, A. G. Borisov, and P. Roncin, Phys. Rev. Lett. **112**, 023203 (2014).
[19] D. E. Chang, K. Sinha, J. M. Taylor, and H. J. Kimble, arXiv:1310.5970v1.
[20] T. Baluktsian, C. Urban, T. Bublat, H. Giessen, R. Löw, and T. Pfau, Opt. Lett. **35**, 1950 (2010).
[21] V. Sandoghdar, C. I. Sukenik, E. A. Hinds, and S. Haroche, Phys. Rev. Lett. **68**, 3432 (1992).
[22] C. I. Sukenik, M. G. Boshier, D. Cho, V. Sandoghdar, and E. A. Hinds, Phys. Rev. Lett. **70**, 560 (1993).
[23] F. Shimizu, Phys. Rev. Lett. **86**, 987 (2001).
[24] V. Druzhinina and M. DeKieviet, Phys. Rev. Lett. **91**, 193202 (2003).
[25] T. A. Pasquini, Y. Shin, C. Sanner, M. Saba, A. Schirotzek, D. E. Pritchard, and W. Ketterle, Phys. Rev. Lett. **93**, 223201 (2004).
[26] H. Bender, P. W. Courteille, C. Marzok, C. Zimmermann, and S. Slama, Phys. Rev. Lett. **104**, 083201 (2010).
[27] A. Landragin, J.-Y. Courtois, G. Labeyrie, N. Vansteenkiste, C. I. Westbrook, and A. Aspect, Phys. Rev. Lett. **77**, 1464 (1996).
[28] A. K. Mohapatra and C. S. Unnikrishnan, Europhys. Lett. **73**, 839 (2006).
[29] R. E. Grisenti, W. Schöllkopf, J. P. Toennies, G. C. Hegerfeldt, and T. Köhler, Phys. Rev. Lett. **83**, 1755 (1999).
[30] J. D. Perreault and A. D. Cronin, Phys. Rev. Lett. **95**, 133201 (2005).
[31] M. Oria, M. Chevrollier, D. Bloch, M. Fichet, and M. Ducloy, Europhys. Lett. **14**, 527 (1991).
[32] I. Hamdi, P. Todorov, A. Yarovitski, G. Dutier, I. Maurin, S. Saltiel, Y. Li, and A. Lezama, Laser Phys. **15**, 987 (2005).
[33] M. Fichet, G. Dutier, A. Yarovitsky, P. Todorov, I. Hamdi, I. Maurin, S. Saltiel, D. Sarkisyan, M.-P. Gorza, D. Bloch, and M. Ducloy, Europhys. Lett. **77**, 54001 (2007).
[34] A. Laliotis, I. Maurin, P. Todorov, I. Hamdi, G. Dutier, A. Yarovitski, S. Saltiel, M.-P. Gorza, M. Fichet, M. Ducloy, and D. Bloch, Proc. SPIE Int. Soc. Opt. Eng. **6604**, 660406 (2007).
[35] A. P. Mosk, M. W. Reynolds, T. W. Hijmans, and J. T. M. Walraven, Phys. Rev. Lett. **81**, 4440 (1998).
[36] L. Weller, R. J. Bettles, P. Siddons, C. S. Adams, and I. G. Hughes, J. Phys. B **44**, 195006 (2011).
[37] J. Keaveney, A. Sargsyan, U. Krohn, I. G. Hughes, D. Sarkisyan, and C. S. Adams, Phys. Rev. Lett. **108**, 173601 (2012).
[38] G. Dutier, S. Saltiel, D. Bloch, and M. Ducloy, J. Opt. Soc. Am. B **20**, 793 (2003).
[39] J. Keaveney, Ph.D. thesis, Durham University, 2013, http://etheses.dur.ac.uk/7748/.
[40] P. Siddons, C. S. Adams, C. Ge, and I. G. Hughes, J. Phys. B **41**, 155004 (2008).
[41] J. Keaveney, I. G. Hughes, A. Sargsyan, D. Sarkisyan, and C. S. Adams, Phys. Rev. Lett. **109**, 233001 (2012).
[42] L. Weller, T. Dalton, P. Siddons, C. S. Adams, and I. G. Hughes, J. Phys. B **45**, 055001 (2012).
[43] L. Weller, K. S. Kleinbach, M. a. Zentile, S. Knappe, C. S. Adams, and I. G. Hughes, J. Phys. B **45**, 215005 (2012).
[44] M. a. Zentile, R. Andrews, L. Weller, S. Knappe, C. S. Adams, and I. G. Hughes, J. Phys. B **47**, 075005 (2014).
[45] A. Derevianko, W. R. Johnson, M. S. Safronova, and J. F. Babb, Phys. Rev. Lett. **82**, 3589 (1999).
[46] B. Arora and B. K. Sahoo, Phys. Rev. A **89**, 022511 (2014).
[47] I. G. Hughes and T. P. A. Hase, *Measurements and their Uncertainties: A Practical Guide to Modern Error Analysis* (OUP, Oxford, 2010).
[48] E. G. Lima, M. Chevrollier, O. Di Lorenzo, P. C. Segundo, and M. Oria, Phys. Rev. A **62**, 013410 (2000).
[49] A. H. Safavi-Naeini, S. Gröblacher, J. T. Hill, J. Chan, M. Aspelmeyer, and O. Painter, Nature (London) **500**, 185 (2013).